Mode-mode interaction for a CO_2 laser with imperfect O(2) symmetry

R. López Ruiz, G. B. Mindlin, and C. Pérez García
Universidad de Navarra, Departamento de Física y Matemática Aplicada, Pamplona 31080, Navarra, Spain

Jorge Tredicce
Institute Non Lineaire de Nice, F06034, Nice Cedex, France
(Received 8 June 1992; revised manuscript received 20 August 1992)

The nonlinear interaction between transverse modes bifurcating from the trivial solution is studied for a CO_2 laser with "imperfect" O(2) symmetry. The modes considered in this work are the Gaussian mode and the ones with angular momentum ± 1. Solutions qualitatively different than the ones present in the perfect case are found, which are in agreement with the ones observed [E.J. D'Angelo *et al.*, Phys. Rev. Lett. **68**, 3702 (1992)] in recent experiments.

PACS number(s): 42.65.Pc, 02.20.−a, 42.55.Lt

I. INTRODUCTION

There is a growing interest in the study of complex spatial temporal behavior in physical systems. Actually the origin and characterization of turbulence might be the oldest unsolved problem in physics. It is now widely known that lasers can be present complex self-pulsing due to the nonlinear interaction of the electromagnetic field and the active atoms in the cavity. More recent studies indicate that lasers can also exhibit complex spatial structures, and there is hope that they will become a useful test bench for turbulence theories [1–3].

Although most practical lasers operate with a simple Gaussian transverse intensity distribution, it is possible to achieve situations where many transverse modes are active. The nonlinear coupling between these modes gives rise to complicated dynamics, as shown by Green *et al.* [4]. In their work, the theory of bifurcations in the presence of symmetries was used in order to understand the appearance of traveling and standing waves leading toward spatiotemporal complexity in the transverse patterns of the intensity of a CO_2 laser. It was assumed that the system had a perfect O(2) symmetry (imposed by the cylindrical laser tube) and that two modes were interacting nonlinearly. There was a qualitative agreement between the solutions found experimentally and some of the solutions predicted by the theory of bifurcations in the presence of symmetries [5]. This theory predicts the existence of solutions with certain symmetries, but not their stability. Therefore, a more quantitative agreement requires the computation of the coefficients of the normal forms for the bifurcation under study from a physical model (in this case, from the Maxwell-Bloch equations). According to the theory of bifurcations in the presence of symmetries, a first bifurcation leading toward a traveling wave was as likely to occur as a bifurcation toward a standing wave. The experimental evidence indicated a preference for standing waves [4,1]. Unfortunately, the Maxwell-Bloch equations with circular boundary conditions predict that a bifurcation that gives birth to a solution breaking the O(2) symmetry will give us *stable traveling waves* and unstable standing waves [6].

In order to explain the appearance of stable standing waves in that experiment, we suggested that the symmetry of the problem might be an "imperfect" O(2) symmetry [1]. Physically this means that although the cavity imposes an O(2) symmetry to the problem (rotations and reflections), there are anisotropies in some of the laser parameters (e.g., the gain, the losses, the pumping) that break the symmetry. Mathematically we say that a problem has an imperfect O(2) symmetry if the equations that describe it can be written as an O(2) equivariant term plus a perturbation that is not equivariant under O(2). Specifically we propose a perturbation equivariant under Z_2 (reflections). As Z_2 is a subgroup of O(2), the problem has a Z_2 symmetry [7].

These ideas were tested for an "annulus" laser [1]. It consisted of a CO_2 laser in which the interaction between the electromagnetic field and the atoms in the cavity can take place only in a narrow range of values in the radial coordinates. This was experimentally achieved with an intracavity iris. The only spatial variable then was the angle θ, with periodic boundary conditions. This configuration allowed the comparison with theoretical results worked out by Dangelmayr and Knobloch [7], who were the first, we believe, to study the appearance of modes with nontrivial angular dependence through Hopf bifurcations in the presence of imperfect symmetries.

If the interaction of field and atoms is allowed everywhere in the tube, though, the modes that break the circular symmetry do not generically appear from a vanishing electric field; usually the first mode to be born is the Gaussian transverse mode [6]. In this paper we study the nonlinear interaction between the Gaussian mode with nonsymmetric modes for a laser with imperfect symmetry. We find solutions that cannot be found in a perfectly symmetric system and are in agreement with recent experiments [1].

II. MODEL

Solari and Gilmore studied the conditions necessary to obtain primary bifurcation branches from the trivial solution for a CO_2 laser with perfect O(2) symmetry [6]. The system under study was a laser in a Fabry-Pérot cavity. The cavity had a perfectly reflecting mirror at one end and a reflecting spherical mirror at the other. Experimentally, the change of the curvature of this last mirror can be achieved by inserting a passive optical device in the cavity. The pumping and the curvature of the mirror were the parameters varied in their theoretical study, in correspondence with the experimental situation.

Under these conditions the electric field can be written as

$$E=P_1(r)L_1(l)(z_1e^{i\theta}+z_2e^{-i\theta})e^{i\omega_1 t} + P_0(r)L_0(l)z_0e^{i\omega_0 t} , \quad (1)$$

where $P_{0,1}$ are the radially dependent parts of the bifurcating modes, and $L_{0,1}$ the longitudinal ones. The action of the O(2) group on the amplitudes is given by

$$\Theta(z_1,z_2,z_0)=(e^{i\theta}z_1,e^{-i\theta}z_2,z_0) , \quad (2)$$

$$K(z_1,z_2,z_0)=(z_2,z_1,z_0) , \quad (3)$$

where Θ and K represent the rotation and reflection operations, respectively. Introducing this electric field into the Maxwell-Bloch equations, and keeping terms to third order, they got the following vector field for the amplitude of the modes:

$$z_1'=\lambda_1 z_1-[A(z_1z_1^*+2z_2z_2^*)+Dz_0z_0^*]z_1 , \quad (4)$$

$$z_2'=\lambda_1 z_2-[A(2z_1z_1^*+z_2z_2^*)+Dz_0z_0^*]z_2 , \quad (5)$$

$$z_0'=\lambda_0 z_0-[E(z_1z_1^*+z_2z_2^*)+Bz_0z_0^*]z_0 , \quad (6)$$

where $\lambda_{0,1}=\lambda_{0,1}^r+i\lambda_{0,1}^i$ are functions of the detunings, the parameters that characterize the pumping profile, and the reflectivity of the mirror. The coefficients A,B,E,D are basically convolutions of the spatial part of the modes with the pumping profile. It is worthwhile to notice that the real part of these coefficients are positive quantities (see Appendix).

The solutions that are obtained for this system are briefly reviewed in the following section, but there is a feature to be stressed here. The solutions with $z_1=z_2$ (standing waves) are *unstable* and the solutions with either z_1 or $z_2=0$ (rotating waves) are stable. This is a discrepancy with the experiment, as there is a clear preference for standing waves (which are observed as sets of "balls" in the averaged intensity). Notice that the stability of the rotating waves and the instability of the standing wave is due to the fact that the ratio between the coefficients of the terms $z_1z_1^*$ and $z_2z_2^*$ is 2, and does not depend on the particular values of the coefficients.

In order to explain this discrepancy we assume that there is an asymmetry in the pumping profile, which acts linearly on the electric field. The pumping is usually introduced phenomenologically in the model, and a symmetry is conjectured for simplicity. It is often assumed to be a Gaussian function $K(r)=ke^{-cr^2}$, where c is the order of (radius of the tube)$^{-1}$. If we now include a perturbation term proportional to $\cos^2(\theta)$, the equations for z_1 and z_2 will couple (see Appendix). Such a term would take into account the existence of physical asymmetries, giving rise to a "privileged" direction. The equations will now read

$$z_1'=\lambda_1 z_1-[A(z_1z_1^*+2z_2z_2^*)+Dz_0z_0^*]z_1+\epsilon z_2 + \epsilon' z_0z_2^*z_2+\epsilon''(z_1z_2^*+z_1^*z_2)z_1 , \quad (7)$$

$$z_2'=\lambda_1 z_2-[A(2z_1z_1^*+z_2z_2^*)+Dz_0z_0^*]z_2+\epsilon z_1 + \epsilon' z_0z_2^*z_1+\epsilon''(z_1z_2^*+z_1^*z_2)z_2 , \quad (8)$$

$$z_0'=\lambda_0 z_0-[E(z_1z_1^*+z_2z_2^*)+Bz_0z_0^*]z_0 + \epsilon''(z_1z_2^*+z_1^*z_2)z_0 . \quad (9)$$

Notice that now the system is no longer equivariant under rotation, and only the Z_2 symmetry remains. From a mathematical point of view, the terms that break the SO(2) symmetry will couple the equations of the modula of the z_i with the phase difference between z_1 and z_2, and therefore will be responsible for qualitative changes in the solutions of the system. Notice that the strongest effects will come from the linear terms in z_1,z_2. Therefore we will take hereafter $\epsilon',\epsilon''=0$ [7].

Letting $z_i=\rho_i e^{i\phi_i}$ and scaling, this system may now be conveniently written as

$$\rho_1'=\lambda_1^r\rho_1-a^r(\rho_1^2+2\rho_2^2)\rho_1+\rho_\epsilon\rho_2\cos(\delta+\phi_\epsilon)-\rho_0^2\rho_1 , \quad (10)$$

$$\rho_2'=\lambda_1^r\rho_2-a^r(2\rho_1^2+\rho_2^2)\rho_2+\rho_\epsilon\rho_1\cos(\delta-\phi_\epsilon)-\rho_0^2\rho_2 , \quad (11)$$

$$\rho_0'=\lambda_0^r\rho_0-(\rho_1^2+\rho_2^2)\rho_0-b^r\rho_0^3 , \quad (12)$$

$$\delta'=-a^i(\rho_1^2-\rho_2^2)-[\rho_1/\rho_2\sin(\delta-\phi_\epsilon) + \rho_2/\rho_1\sin(\delta+\phi_\epsilon)]\rho_\epsilon , \quad (13)$$

and

$$\phi_1'=\lambda_1^i-a^i(\rho_1^2+2\rho_2^2)+\rho_\epsilon\rho_2/\rho_1\sin(\delta+\phi_\epsilon)-d^i\rho_0^2 , \quad (14)$$

$$\phi_0'=\lambda_0^i-e^i(\rho_1^2+\rho_2^2)-b^i\rho_0^2 , \quad (15)$$

where $\delta=\phi_2-\phi_1$, $a^r=A^r/E^r$, $a^i=A^i/E^r$, and $b^r=B^r/D^r$, $b^i=B^i/D^r$, $d^i=D^i/D^r$, $e^i=E^i/E^r$. Now the system is ruled by a subset of only four equations, $\phi_{0,1}$ being enslaved by the others.

This set of equations is an extension to the case of three modes of the one studied by Dangelmayr and Knobloch [7], who analyzed the appearance of the modes $e^{+i\theta},e^{-i\theta}$ in the presence of a Z_2 symmetry degenerated towards O(2), as in this case. They can also be thought of as an extension to the imperfect case of the equations with perfect symmetry studied by Solari and Gilmore [6].

III. SOLUTIONS

In the case of perfect symmetry, the equations are particularly easy, as the equations for the amplitude decouple from the equations of the phases. In Fig. 1 we show the unfolding of the Hopf-Hopf bifurcation displaying different solutions in the (ρ_1,ρ_2,ρ_0) projection of the phase space for different values of the two unfolding pa-

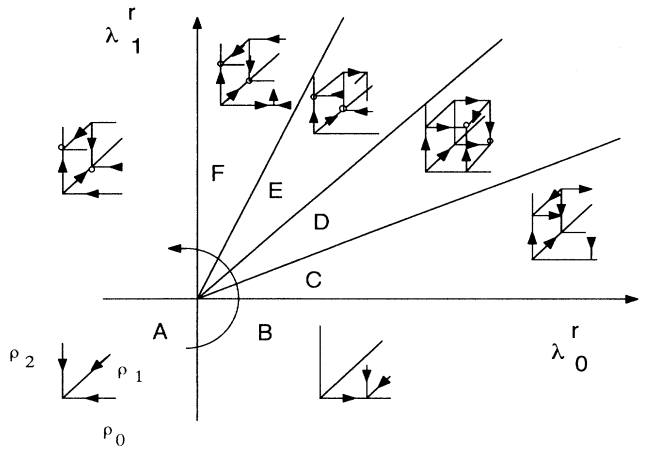

FIG. 1. Unfolding of the Hopf-Hopf bifurcation in the case of perfect symmetry. The open circles indicate the position in the (ρ_0,ρ_1,ρ_2) projection of the phase space of the stable traveling waves. This figure is an adaptation of Fig. 5 in [6].

rameters. It is generic, for the case of the laser, to turn on the Gaussian mode first. Therefore we will briefly describe the solutions expected for this problem following the curved arrow shown in Fig. 1. We begin with the trivial solution (region of the unfolding parameter space labeled A in Fig. 1), which loses stability in a Hopf bifurcation as $\mathrm{Re}(\lambda_0)>0$ (region B). As $\mathrm{Re}(\lambda_1)$ becomes also positive, the zero solution emits two traveling waves (TW) (saddle) and a standing wave (SW) (unstable) both with $\rho_0=0$ (region C). Then the $(0,0,\rho_0)$ solution emits two attracting TW and a SW with $\rho_0\langle\ \rangle 0$ (region D). As the parameters are further changed as indicated by the arrow, these TW collide with the unstable TW at $\rho_0=0$ (region E). The SW with $\rho_0\langle\ \rangle 0$ also collides with the unstable SW with $\rho_0=0$ (region F). From all this description it is important to emphasize that the TW are the only stable solutions when the symmetry is not broken.

If the symmetry-breaking terms are included, there will be qualitative changes in the solutions. For convenience let us introduce another change of variables. If

$$\rho_1 = A\cos(\phi/2)\ , \tag{16}$$

$$\rho_2 = A\sin(\phi/2)\ , \tag{17}$$

Eqs. (10)–(15) will now read

$$A' = \{\lambda_1^r - a^r[1+\tfrac{1}{2}\sin^2(\phi)]A^2\}A + [\rho_\epsilon\sin(\phi)\cos(\delta)\cos(\phi_\epsilon) - \rho_0^2]A\ , \tag{18}$$

$$\phi' = -\tfrac{1}{2}a^r\sin(2\phi)A^2 + 2\rho_\epsilon[\cos(\phi_\epsilon)\cos(\delta)\cos(\phi) + \sin(\phi_\epsilon)\sin(\delta)]\ , \tag{19}$$

$$\delta' = -a^i A^2\cos(\phi) + \rho_\epsilon[\mathrm{cotan}(\phi/2)\sin(\phi_\epsilon-\delta) - \tan(\phi/2)\sin(\phi\epsilon+\delta)]\ , \tag{20}$$

$$\rho_0' = \lambda_0^r\rho_0 - A^2\rho_0 - b^r\rho_0^3\ . \tag{21}$$

In the $(\rho_0=0)$ subspace we have solutions for $\phi=\pi/2$, $\delta=0,\pi$ with amplitude

$$A^2 = \tfrac{2}{3}[\lambda_1^r \pm \rho_\epsilon\cos(\phi_\epsilon)]/a^r\ , \tag{22}$$

where the + (−) corresponds to the solution with $\delta=0$ (π). Hereafter this solution will be called SW_0^0 (SW_π^0). If $\phi_\epsilon\in[-\pi/2,\pi/2]$ $([\pi/2,3\pi/2])$, the first solution to bifurcate (as λ_1^r is increased, for a fixed value of ρ_ϵ) is the one with $\delta=0$ (π). As

$$E = (z_1e^{i\theta} + z_2e^{-i\theta})f(r)e^{i\omega t} \tag{23}$$

$$= e^{i\phi_1}\rho(e^{i\theta} + e^{-i(\theta-\delta)})e^{i\omega t}f(r) \tag{24}$$

$$= \rho e^{i(\phi+\delta/2)}(e^{i(\theta-\delta/2)} + e^{-i(\theta-\delta/2)})e^{i\omega t}f(r)\ , \tag{25}$$

the averaged intensity pattern for the solution with $\delta=0$ (π) will look like a set of two intense spots aligned with (perpendicular to) the privileged axis [see Figs. 2(a) and 2(b)].

The stability of these standing waves can be computed as a function of λ_1^r, ρ_ϵ, and ϕ_ϵ. The eigenvalue associated to the A direction is $-2[\lambda_1^r \pm \rho_\epsilon\cos(\phi_\epsilon)]$, while the eigenvalues associated to the ϕ and δ directions are the eigenvalues of the Jacobian

$$J_{DF} = \begin{bmatrix} \tfrac{2}{3}\lambda_1^r \pm \dfrac{-4}{3}\rho_\epsilon\cos(\phi_\epsilon) & \pm 2\rho_\epsilon\sin(\phi_\epsilon) \\ \tfrac{2}{3}(a^i/a^r)[\lambda_1^r \pm \rho_\epsilon\cos(\phi_\epsilon)] \mp 2\rho_\epsilon\sin(\phi_\epsilon) & \mp 2\rho_\epsilon\cos(\phi_\epsilon) \end{bmatrix}\ . \tag{26}$$

Studying the behavior of these eigenvalues in the $(\rho_\epsilon,\lambda_1^r)$ parameter space for different fixed values of ϕ_ϵ, we can state that for $\phi_\epsilon\in[-\pi/2,\pi/2]$ $([\pi/2,3\pi/2])$ there will be an interval in λ_1^r such that SW_0^0 (SW_π^0) is stable. In this model, that interval grows with ρ_ϵ. Moreover, once that λ_1^r takes values such that SW_0^0 (SW_π^0) exists as a stable solution, it cannot become unstable as ρ_ϵ is increased (see Fig. 3). One has to keep in mind though that the limit $\rho_\epsilon\to\infty$ is beyond the scope of this model. The reason is that A increases with ρ_ϵ, and we truncated the normal forms to third order.

For a fixed value of ρ_ϵ, increasing λ_1^r will induce secondary bifurcations from the standing waves. The kind of solutions obtained after the bifurcations depends on the value of ϕ_ϵ. As we already mentioned, for $\phi_\epsilon\in[-\pi/2,\pi/2]$ $([\pi/2,3\pi/2])$ there is a range of values of λ_1^r for which SW_0^0 (SW_π^0) is stable. If $\phi_\epsilon\in[\pi/2-\alpha,\pi/2]$ or $[3\pi/2,3\pi/2+\alpha]$ $([\pi/2,\pi/2+\alpha]$ or $[3\pi/2-\alpha,3\pi/2])$ the SW_0^0 (SW_π^0) bifurcates to a modulated wave in a Hopf bifurcation (the value of α de-

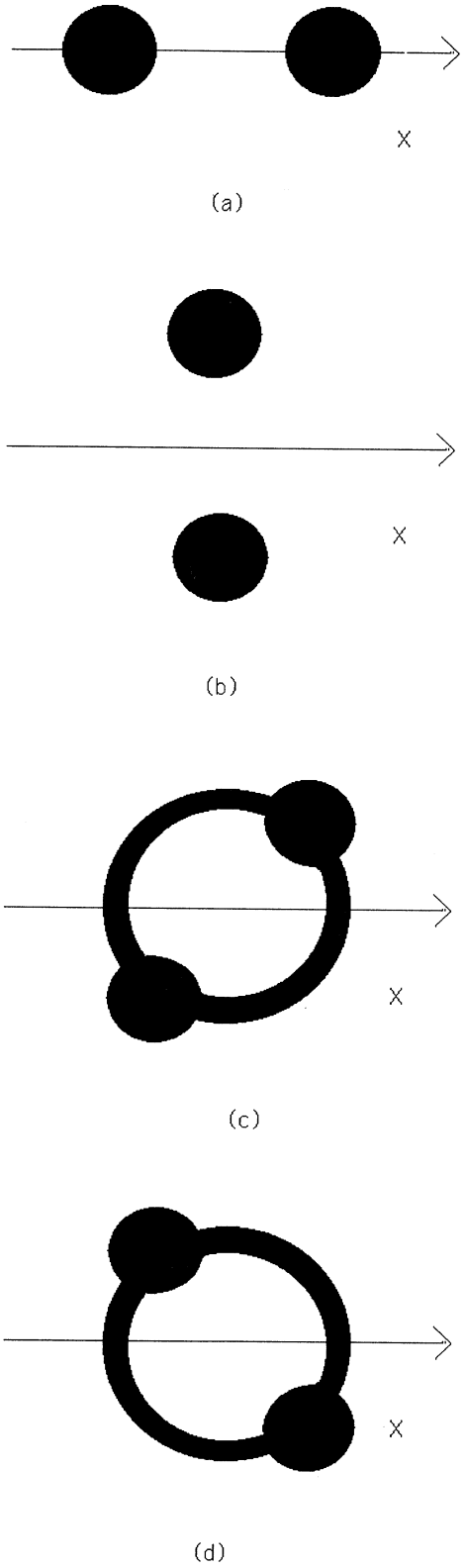

FIG. 2. Averaged intensity for SW_0^0 (a), for SW_π^0 (b) and for the TW′ solutions $(\rho_1^*,\rho_2^*,\pi+\delta^*,0)$ (c) and $(\rho_2^*,\rho_1^*,\pi-\delta^*,0)$ (d). The line represents the privileged axis that breaks the O(2) symmetry.

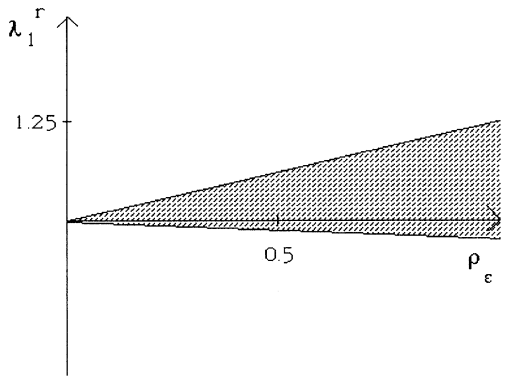

FIG. 3. Stability region of SW_π^* for $\phi_\epsilon=1.82$, $\lambda_0^r<0$, in the $(\rho_\epsilon,\lambda_1^r)$ space. According to this model, once a SW gains stability, it will not lose it as ρ_ϵ is increased.

pends on a_i/a_r; for $a_i=0$, $\alpha=\pi/4$). Otherwise, the SW_0^0 (SW_π^0) bifurcates to two solutions $(A^*,\pi/2\pm\beta^*,\pm\delta^*)$ $[A^*,\pi/2\pm\beta^*,\pi\pm\delta^*)]$ in a pitchfork bifurcation. These solutions are a mixture of traveling waves and standing waves and will be called hereafter (TW′). Proceeding as in Eq. (23)–(25) one finds that the TW′ solutions have an averaged intensity as the one displayed in Figs. 2(c) and 2(d).

If λ_0^r is increased, SW_0^0 (SW_π^0) loses stability in the ρ_0 direction. If $\phi=\pi/2$, $\delta=0(\pi)$, Eqs. (18)–(21) become

$$\rho_0'=(\lambda_0-A^2-b^r\rho_0^2)\rho_0 , \tag{27}$$

$$A'=\{[\lambda_0^r\pm\rho_\epsilon\cos(\phi_\epsilon)]-\tfrac{3}{2}a^rA^2-\rho_0^2\}A . \tag{28}$$

Therefore there will be fixed points outside the axes if

$$\lambda_0^r-A^2-b^r\rho_0^2=0 , \tag{29}$$

$$\lambda_1^r\pm\rho_\epsilon\cos(\phi_\epsilon)-\tfrac{3}{2}a^rA^2-\rho_0^2=0 . \tag{30}$$

If $1-\frac{3}{2}a^rb^r(\ )0$,

$$\begin{bmatrix} A^2 \\ \rho_0^2 \end{bmatrix}=\frac{1}{1-\frac{3}{2}a^rb^r}\begin{bmatrix} 1 & -b^r \\ -\frac{3}{2}a^r & 1 \end{bmatrix}\begin{bmatrix} \lambda_0^r \\ \lambda_1^r\pm\rho_\epsilon\cos(\phi_\epsilon) \end{bmatrix} . \tag{31}$$

If $A^2,\rho_0^2>0$ there will be a fixed point outside the axes. This implies that if $1-\frac{3}{2}a^rb^r>0$ (<0), the fixed point will exist if

$$\lambda_0^r-b^r[\lambda_1^r\pm\rho_\epsilon\cos(\phi_\epsilon)]>0(<0) , \tag{32}$$

$$-\tfrac{3}{2}a^r\lambda_0+[\lambda_1^r\pm\rho_\epsilon\cos(\phi_\epsilon)]>0(<0) . \tag{33}$$

Notice that for a given λ_1^r, a large ρ_ϵ implies a large λ_0^r range in which these standing waves exist. But as we mentioned before, the limit of large ρ_ϵ is beyond the scope of this model.

With this analytical "skeleton" in mind, we are interested in studying the complete two-dimensional unfolding of this nonlinear interaction between the Gaussian and the $e^{\pm i\theta}$ modes. As in the experiments, the presence of modulated waves was reported; we will choose for

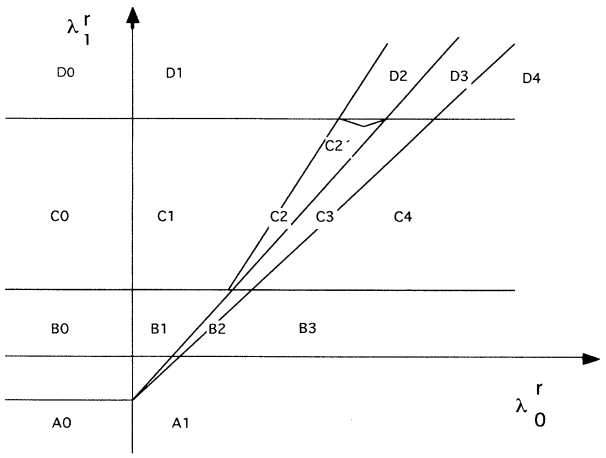

FIG. 4. Unfolding of the Hopf-Hopf bifurcation in the case of imperfect symmetry. The values of a^r and b^r were taken as 1. A change in these values results in a change of the relative sizes of the regions, but not in the qualitative features of the solutions.

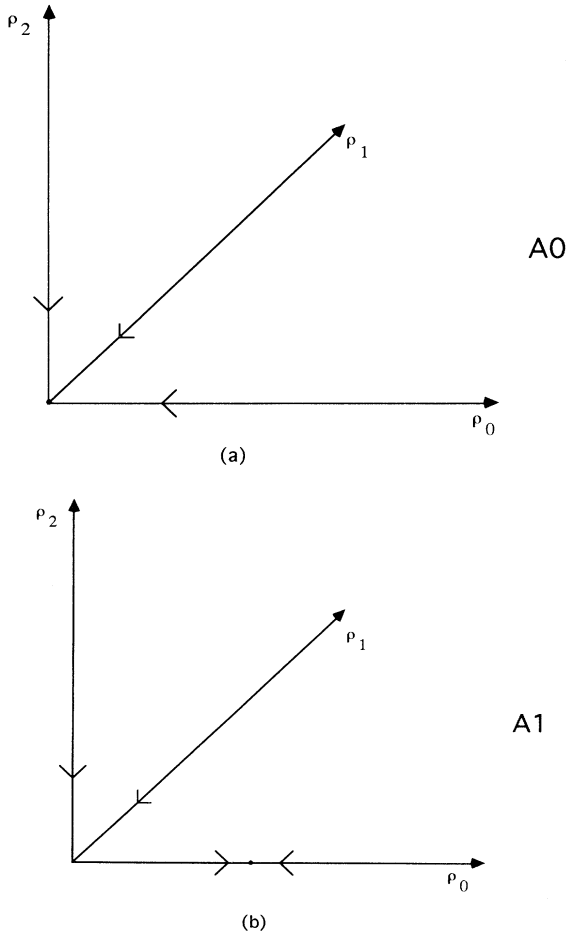

FIG. 5. Phase-space behavior for the A region of parameter space. (a) displays the behavior for the A0 region, and (b) for the A1 region.

our numerical exploration values of ϕ_ϵ such that the standing waves lose stability in a Hopf bifurcation as λ_1^r is increased.

For $\phi_\epsilon = 1.8$ and $\epsilon\epsilon^* = 0.25$, we studied the two-dimensional unfolding in a similar way to the perfect case. Figure 4 summarizes the results. The "core" system, being four dimensional, urges us to choose three-

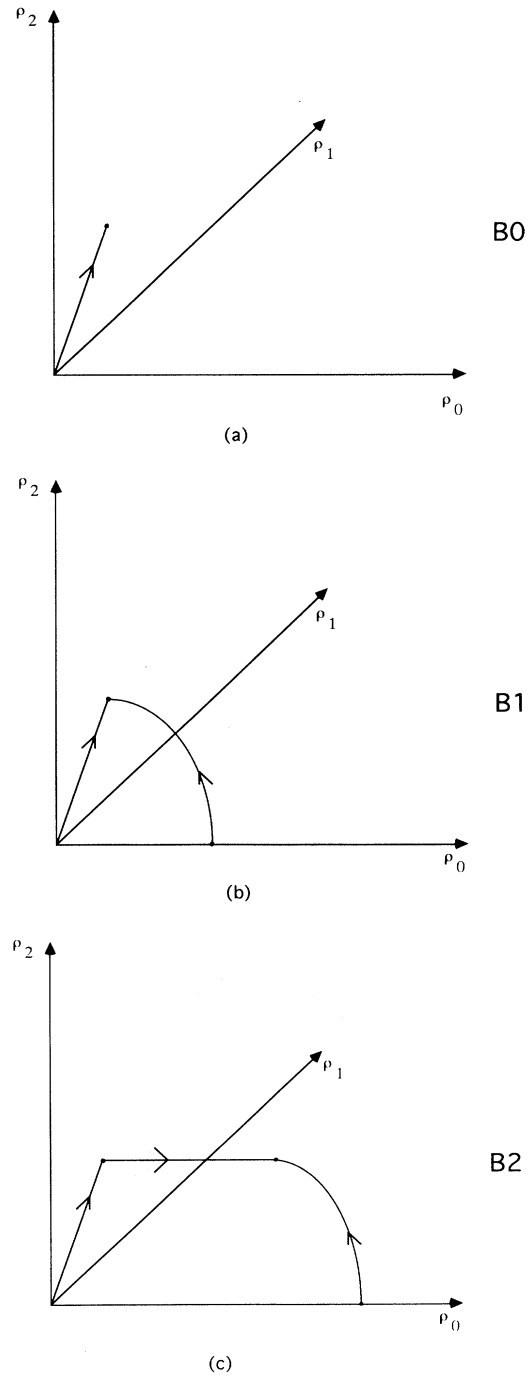

FIG. 6. Phase-space behavior for the B0 region (a), the B1 region (b), and the B2 region (c).

dimensional projections in order to describe with figures the different phase-space behaviors found for different values of the parameters (Figs. 5–8). We choose to project on (ρ_1,ρ_2,ρ_0) to make the comparison with the perfect case (Fig. 1) easier.

We begin our description as the region indicated by A0 in Fig. 4. The zero solution is stable. As the parameter λ_1^r is increased, the zero solution loses stability towards a standing wave SW_π^0 (region B0 in parameter space). Its averaged intensity profile is shown in Fig. 9(a). It consists basically of two symmetric bright spots. If we increase λ_1^r even further, this solution loses stability through a Hopf bifurcation, creating a stable modulated wave hereafter called MW_π^0 (region C0). Increasing λ_1^r

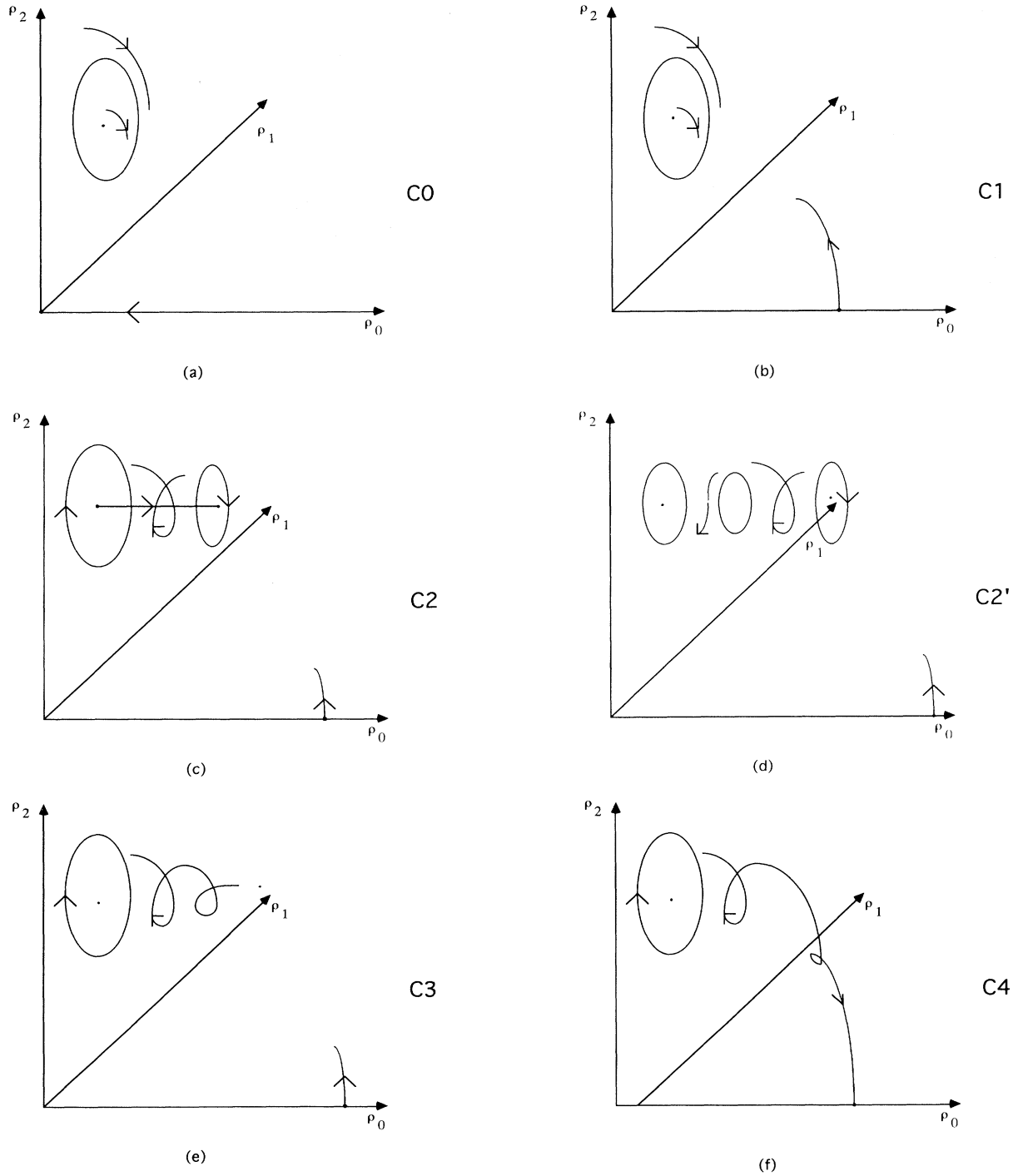

FIG. 7. Phase-space behavior for the C0 region (a), C1 region (b), C2 region (c), C2′ region (d), C3 region (e), and C4 region (f). Notice the coexistence of stable MW_0 and MW′ in region C2′.

even further (region D0), two saddle node bifurcations occur *in the limit cycle,* giving rise to TW′ solutions. Notice that before reaching the λ_1^r value for which the bifurcation takes place, there is a critical slowing down of the MW_π^0 in the neighborhood of the regions of phase space in which these fixed points will appear. The observable consequence of this dynamical behavior will be the periodic alternancy between patterns as the ones shown in Figs. 2(c) and 2(d).

If we increase λ_0^r beginning at region B we observe the following. When λ_0^r becomes positive, the Gaussian mode is born. This solution has an unstable manifold that feeds the standing wave. If λ_0^r is increased even further, the standing wave emits a solution (ρ,ρ,ρ_0,π) (region B2) that collapses with the Gaussian solution at region B3.

Beginning at region C0 and increasing λ_0^r we observe the following. At $\lambda_0^r=0$, the Gaussian mode is born. As before, its unstable manifold feeds the modulated wave that lives at $\rho_0=0$. At region C2 we observe a stable modulated wave with $\rho_0\langle\ \rangle 0$ (hereafter MW_π'), which emitted by the MW_π^0 [see Fig. 9(b)] and a standing wave (ρ,ρ,ρ_0,π), which was emitted by the SW_π^0.

The MW_π' is a rather interesting solution, as three frequencies are to be found anywhere in the intensity pattern. Its average intensity profile is shown in Fig. 9(b). It consists of a nonhomogeneous bright ring. If the amplitude of the limit cycle bifurcating from the SW is small, the nonhomogeneities will look like the symmetric spots of Fig. 9(a), and the ring will hardly be noticed. This solution collapses with the (ρ,ρ,ρ_0,π) solution at an inverse Hopf bifurcation (region C3), and the former collapses with the Gaussian mode at region C4.

It is worthwhile to describe what happens to regions C0, C1, C2, C3 as λ_1^r is increased. We already said that if we increase λ_1^r from region C0 we have a saddle node bifurcation taking place at the limit cycle MW_π^0. Increasing λ_1^r from C1 and C2 simply produces the same effect. From C3 to $C2'$, though, a rather interesting phenomenon takes place. The modulated wave MW_π^0 emits an unstable modulated wave with $\rho_0\langle\ \rangle 0$ gaining stability [Fig. 7(d)]. Therefore, we have the coexistence of two stable modulated waves. As λ_1^r is further increased, the modulated wave MW_π^0 breaks as described before giving rise to a coexistence between a stable modulated wave

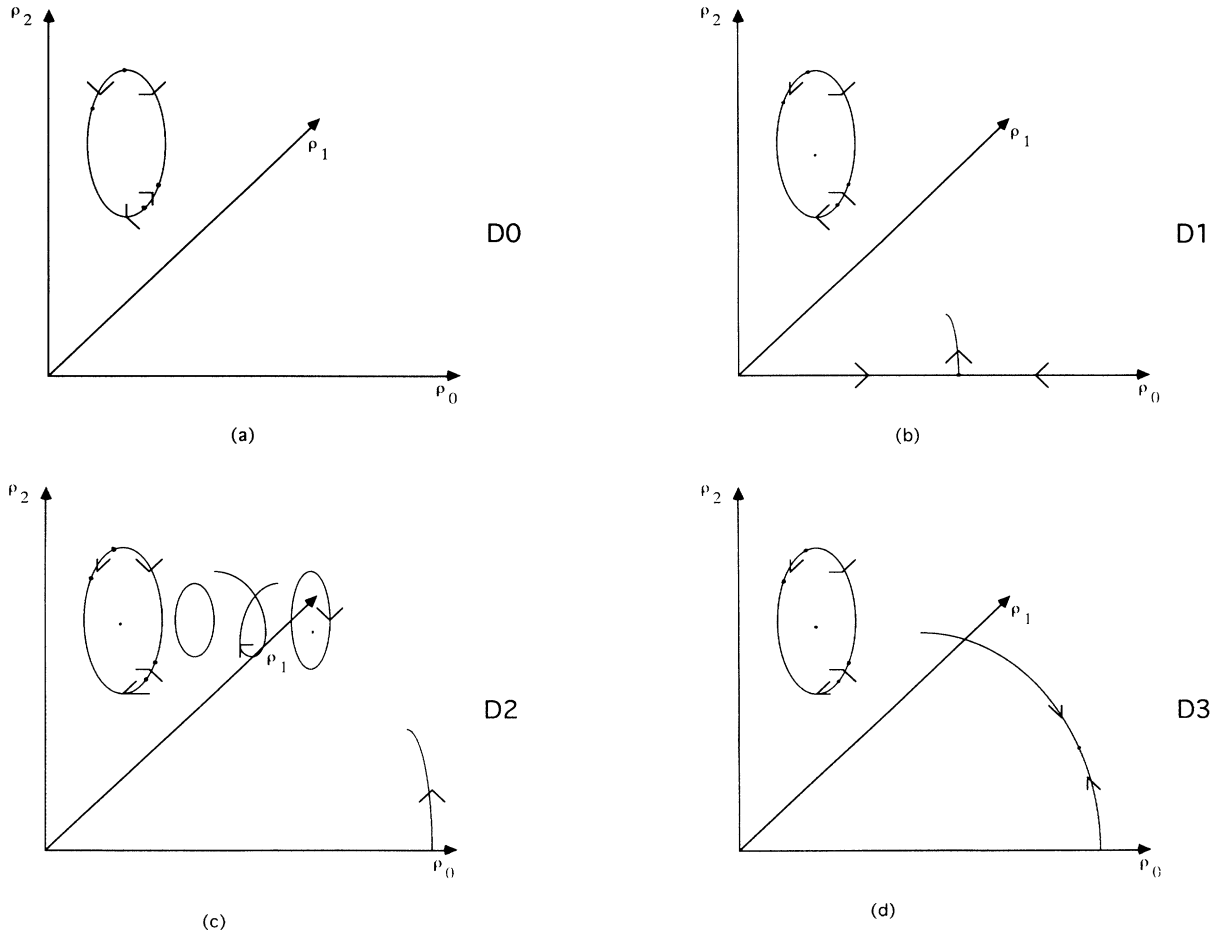

FIG. 8. Phase-space behavior for the D0 region (a), D1 region (b), D2 region (c), and D3 region (d). Notice the coexistence between stable TW′ and MW′ solutions in region D2.

and two TW' (region D2). Notice that the existence of regions as D2 and C2', where multistability of solutions takes place, implies hysteresis as parameters are changed. The information presented in this section is summarized in Table I.

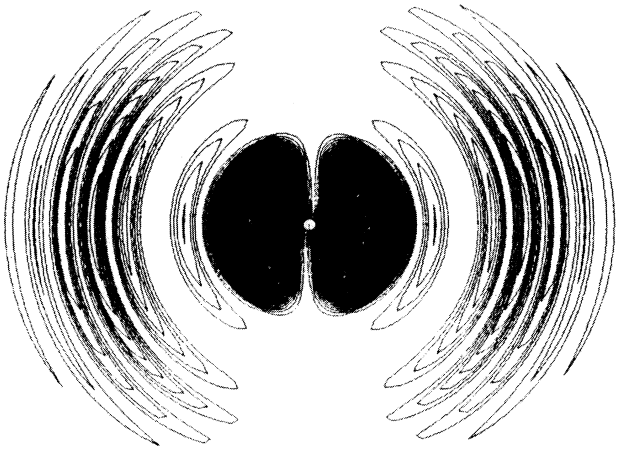

(a)

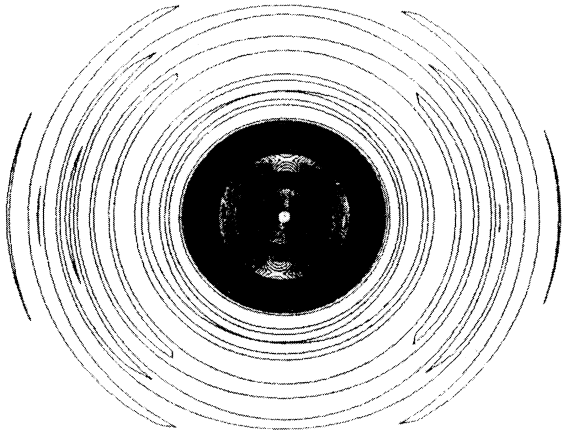

(b)

FIG. 9. Average intensity for the (a) standing wave SW0 and the (b) modulated wave MW'. The MW' is born from a standing wave in a Hopf bifurcation. Therefore for some values of the parameters it has an asymmetry that reminds us of a standing wave. Also notice that as ρ_0 itself oscillates around a nonzero value, the center of the pattern is a bright spot. This solution does not exist for the perfectly O(2) symmetric case.

TABLE I. Summary of the solutions in the $(\lambda_1^r, \lambda_0^r)$ unfolding of the nonlinear interaction between the Gaussian mode and the $e^{\pm i\theta}$ modes described in Sec. III. O stands for the trivial solution, G for the Gaussian solution, SW0 for the SW_π^0 solution (defined in Sec. III), SW' for the standing wave with $\rho_0\langle\ \rangle 0$, TW' for the solutions' mixture between traveling and standing waves, MW^0 for the modulated wave bifurcating from the SW_π^0 solution, and MW' stands for the modulated wave with $\rho_0\langle\ \rangle 0$. The stability of the solutions is indicated between parentheses.

Region	Solutions (stability)
A0	O(s)
A1	O(u),G(s)
B0	SW0(s),O(u)
B1	O(u),SW0(s),G(u)
B2	O(u),SW0(u),SW'(s),G(u)
C0	O(u),SW0(u),MW0(s)
C1	O(u),SW0(u),MW0(s),G(u)
C2	O(u),SW0(u),MW0(u),MW'(s),G(u)
C2'	O(u),SW0(u),SW'(u),MW0(s),MW'1(u),MW'2(s),G(u)
C3	O(u),SW0(u),SW'(s),MW0(u),G(u)
C4	O(u),SW0(u),MW0(u),G(s)
D0	O(u),SW0(u),TW'1(s),TW'2(u),TW'3(s),TW'4(u)
D1	same as D0 and G(u)
D2	same as D1 and MW'1(u), MW'2(s)
D3	same as D1 and SW'(s)

IV. CONCLUSIONS

It is a typical procedure in physics to study a phenomenon by designing an experiment with the "easiest" conceivable symmetrical setup. This typically makes the life of both the theoretician and the experimentalist easier. But we should not forget that symmetries imply a high mathematical degeneracy. The normal form of a bifurcation for a system with symmetry will have many terms absent; therefore a slight perturbation is likely to change the qualitative solutions to be found.

In this work we report an unfolding of a codimension two, Hopf-Hopf bifurcation in a system with Z_2 symmetry [highly degenerated toward an O(2) symmetry]. An analytical skeleton for primary and secondary bifurcations from the trivial solution was obtained. Particular parameters were chosen for a deeper numerical description of the unfolding so that the phenomenology would correspond to the one observed in the experiments. The main features of the solutions of the system under study were as follows.

(i) The stability of the standing waves involving modes of nonzero angular momentum. The average intensity of these solutions will be a set of bright spots. In a perfectly symmetric system, the stable solutions involving modes of nonzero angular momentum are the traveling waves. Their average intensity would be a bright ring.

(ii) The existence of stable solutions' mixture of standing waves and the Gaussian mode. These will have an average intensity consisting of a symmetric bright spot and a set of bright spots around it.

(iii) The existence of stable modulated waves emitted by the standing waves. These solutions will have an average intensity consisting of a set of bright spots connected

by a ring. The time-series data of any point in the pattern will exhibit an additional frequency.

(iv) The existence of stable solutions that are a mixture of traveling waves and standing waves. Their average intensity will consist of a set of bright spots connected through a bright ring.

(v) The existence of a periodic alternancy between the patterns of Figs. 2(c) and 2(d). This occurs for parameter values close to the ones in which TW′ solutions are born in the limit cycle in a global bifurcation. This phenomenon might be dynamically similar to the periodic alternancy reported in [3].

Notice that these solutions cannot be obtained under the assumption of perfect symmetry. We believe that beyond a contribution to the understanding of this particular CO_2 laser, this work might be a challenging invitation to explore the consequences of slightly breaking the symmetry in widely studied symmetric problems.

ACKNOWLEDGMENT

This work has been partially supported by the DGICYT (Spanish Government) under Grant No. PB90-0362.

APPENDIX

In Sec. II we claim that an asymmetry in the pumping profile gives rise to the linear coupling between the equations for z_1 and z_2 (7)–(9). In this appendix we briefly review the structure of the Maxwell-Bloch equations [8] and write the parameter ϵ in terms of laser parameters.

Expanding the electric field, the polarization field, and the population inversion field in terms of longitudinal cavity modes and slowly varying amplitudes Φ, Π, D, and plugging them into the Maxwell-Bloch equations, one gets for the slowly varying amplitudes the following:

$$i\frac{\partial}{\partial t}\begin{bmatrix}\Phi_+\\ \Phi_-\end{bmatrix}=\begin{bmatrix}H^+-i\chi & 0\\ 0 & H^--i\chi\end{bmatrix}\begin{bmatrix}\Phi_+\\ \Phi_-\end{bmatrix}-i\begin{bmatrix}\Pi_+\\ \Pi_-\end{bmatrix}, \tag{A1}$$

$$\begin{bmatrix}\Pi_+\\ \Pi_-\end{bmatrix}=-\begin{bmatrix}D_0 & D_2\\ D_{-2} & D_0\end{bmatrix}\begin{bmatrix}R^+\Phi_+\\ R^-\Phi_-\end{bmatrix}, \tag{A2}$$

$$\left[I_2+1/\gamma\frac{\partial}{\partial t}\right]\begin{bmatrix}D_0 & D_2\\ D_{-2} & D^0\end{bmatrix}=KI_2+\begin{bmatrix}\Phi_+\\ \Phi_-\end{bmatrix}[\Pi_+^* \quad \Pi_-^*]+\begin{bmatrix}\Pi_+\\ \Pi_-\end{bmatrix}[\Phi_+^* \quad \Phi_-^*]$$
$$+[1/(s^2+z^2)]\begin{bmatrix}\Phi_-\Pi_-^*+\Phi_-^*\Pi_- & 0\\ 0 & \Phi_+\Pi_+^*+\Phi_+^*\Pi_+\end{bmatrix}, \tag{A3}$$

$$R^{+-}=(\beta-iH^{+-})^{-1}, \tag{A4}$$

where γ is the rate of decay of the population inversion, β is the atomic rate of decay of the atomic polarization, K is the pumping profile, s is the curvature of the mirrors, and $z=-L+r^2/2A$ (with L the longitudinal size of the tube and A the radius of the mirror).

The trivial solution of these equations is

$$\Phi_{+-}=0, \tag{A5}$$

$$\Pi_{+-}=0, \tag{A6}$$

$$D_{+-2}=0, \tag{A7}$$

and

$$D_0=K. \tag{A8}$$

For certain values of the parameters, different modes are born in Hopf bifurcations. For bifurcation giving rise to the modes we are interested in this work, the normal form can be obtained by plugging

$$\begin{bmatrix}\Phi_+\\ \Phi_-\end{bmatrix}=z_0P_0(r)\begin{bmatrix}L_+^0\\ L_-^0\end{bmatrix} \tag{A9}$$
$$+(z_1e^{i\theta}+z_2e^{-i\theta})]P_1(r)\begin{bmatrix}L_+^1\\ L_-^1\end{bmatrix} \tag{A9}$$

into Eqs. (A1)–(A4). In this way we obtain dynamical equations for the mode amplitudes z_i. For the perfectly symmetric case, this procedure was performed in [6].

Notice that to lowest order, the Π_{+-} are linear in Φ_{+-}

$$\begin{bmatrix}\Pi_+\\ \Pi_-\end{bmatrix}=-\begin{bmatrix}K & 0\\ 0 & K\end{bmatrix}\begin{bmatrix}R^+\Phi_+\\ R^-\Phi_-\end{bmatrix}. \tag{A10}$$

As

$$H^{+-}\begin{bmatrix}L_+^i(l)\\ L_-^i(l)\end{bmatrix}P_i(r)e^{il\theta}=\Omega^i\begin{bmatrix}L_+^i(l)\\ L_-^i(l)\end{bmatrix}P_ie^{il\theta}, \tag{A11}$$

calling

$$\begin{bmatrix}L_+^i(l)\\ L_-^i(l)\end{bmatrix}P_i=|i\rangle \tag{A12}$$

and assuming

$$P_{\text{pumping}}=K(r)+2\alpha\cos(2\theta), \tag{A13}$$

the linear part of the equations for the amplitudes will be

$$
\begin{aligned}
&iz_0'|0\rangle+(iz_1'e^{i\theta}+iz_2'e^{-i\theta})|1\rangle \\
&\quad=-i(\Omega_0-i\chi)z_0|0\rangle-i(\Omega_1-i\chi)(z_1e^{i\theta}+z_2e^{-i\theta})|1\rangle+\frac{1}{\beta-i\Omega_0}Kz_0|0\rangle \\
&\quad+\frac{1}{\beta-i\Omega_1}|1\rangle K(z_1e^{i\theta}+z_2e^{i\theta})+\frac{\alpha}{\beta-i\Omega_1}Ke^{i\theta}z_2|1\rangle+\frac{\alpha}{\beta-i\Omega_1}Ke^{-i\theta}z_1|1\rangle \\
&\quad+e^{2i\theta}(\cdots)+e^{-2i\theta}(\cdots)+e^{3i\theta}(\cdots)+e^{-3i\theta}(\cdots)\ ,
\end{aligned}
\tag{A14}
$$

which implies

$$
iz_0'=\left[\Omega_0-i\chi+i\frac{\langle 0|K|0\rangle}{\beta-i\Omega_0}\right]z_0\ , \tag{A15}
$$

$$
iz_1'=\left[\Omega_1-i\chi+i\frac{\langle 1|K|1\rangle}{\beta-i\Omega_1}\right]z_1+i\frac{\alpha}{\beta-i\Omega_1}z_2\ , \tag{A16}
$$

$$
iz_2'=\left[\Omega_1-i\chi+i\frac{\langle 1|K|1\rangle}{\beta-i\Omega_1}\right]z_2+i\frac{\alpha}{\beta-i\Omega_1}z_1\ . \tag{A17}
$$

Notice therefore that the complex parameter ϵ in equations is

$$
\epsilon=\frac{\alpha}{\beta-i\Omega_1}\ , \tag{A18}
$$

where β (the rate of decay of the atomic polarization) and Ω_1 (the eigenvalue of the empty cavity problem) are of the same order of magnitude.

In order to compute the coefficients of the nonlinear terms one proceeds iteratively [6]. After expanding

$$
\begin{bmatrix}\Phi_+\\ \Phi_-\end{bmatrix}=\sum_\mu z_\mu\begin{bmatrix}a_+^\mu\\ a_-^\mu\end{bmatrix}\ , \tag{A19}
$$

one obtains to lowest order a linear approximation for the polarization. But as the population inversion amplitudes are bilinear functions of these [Eq. (A3)], one gets according to Eq. (A2) that the next lowest order for the polarization is 3. Substituting the third-order approximation to the polarization and the field into Eq. (A1), one can write

$$
z_\alpha'=L_\alpha z_\alpha+M_{\alpha\mu\nu\beta}z_\mu z_\nu^* z_\beta \tag{A20}
$$

with

$$
M_{\alpha\mu\nu\beta}=-G_{\alpha\mu\nu\beta}D_{\alpha\mu\nu\beta}\ , \tag{A21}
$$

where

$$
D_{\alpha\mu\nu\beta}=\frac{1/(\beta-i\Omega_\beta)}{1+i(\Omega_\mu-\Omega_\nu)/\gamma}\left[\frac{1}{\beta-i\Omega_\mu}+\frac{1}{\beta+i\Omega_\nu}\right]\ , \tag{A22}
$$

$$
G_{\alpha\mu\nu\beta}=\int\frac{K}{s^2+z^2}(T^{\alpha\mu}T^{\nu\beta}+T^{\alpha\mu\nu\beta})dv\ , \tag{A23}
$$

$$
T^{\alpha\mu}=(a_+^\alpha)^*a_+^\mu+(a_-^\alpha)^*a_-^\mu\ , \tag{A24}
$$

and

$$
T^{\alpha\mu\nu\beta}=(a_+^\alpha)^*a_+^\mu a_+^{\nu*}a_+^\beta+(a_-^\alpha)^*a_-^\mu a_-^{\nu*}a_-^\beta\ , \tag{A25}
$$

as shown in [6].

[1] E. J. D'Angelo, E. Izaguirre, G. B. Mindlin, G. Huyet, L. Gil, and J. R. Tredicce, Phys. Rev. Lett. **68**, 3702 (1992).

[2] J. R. Tredicce, E. D'Angelo, C. Green, G. B. Mindlin, L. M. Narducci, G. L. Oppo, and H. G. Solari, in *Instabilities and Nonequilibrium Structures III,* edited by E. Tirapegui and W. Zeller (Kluwer Academic, Norwell, 1991), pp. 239–48.

[3] F. T. Arecchi, Physica D **51**, 450 (1991).

[4] C. Green, G. B. Mindlin, E. J. D'Angelo, H. G. Solari, and J. R. Tredicce, Phys. Rev. Lett. **65**, 3124 (1990).

[5] M. Golubitsky, I. Stewart, and D. Schaeffer, *Singularities and Groups in Bifurcation Theory,* Applied Mathematical Sciences Vol. 69 (Springer-Verlag, New York, 1983).

[6] H. G. Solari and R. Gilmore, J. Opt. Soc. Am. B **7**, 828 (1990).

[7] G. Dangelmayr and E. Knobloch, Nonlinearity **4**, 399 (1991).

[8] H. G. Solari and R. Gilmore, Opt. Commun. **71**, 85 (1989).